TU Delft

Delft University of Technology

Document Version
Final published version

Citation (APA)
Song, M., Huang, Y., Shen, Y., Shi, C., Breeschoten, A., Konijnenburg, M., Visser, H., Romme, J., Dutta, B., Alavi, M. S., & More Authors (2022). A 1.66Gb/s and 5.8pJ/b Transcutaneous IR-UWB Telemetry System with Hybrid Impulse Modulation for Intracortical Brain-Computer Interfaces. In L. C. Fujino (Ed.), *2022 IEEE International Solid-State Circuits Conference, ISSCC 2022: Digest of technical papers* (pp. 394-396). Article 9731608 (Digest of Technical Papers - IEEE International Solid-State Circuits Conference; Vol. 2022-February). IEEE.
https://doi.org/10.1109/ISSCC42614.2022.9731608

Important note
To cite this publication, please use the final published version (if applicable).
Please check the document version above.

Copyright
In case the licence states “Dutch Copyright Act (Article 25fa)”, this publication was made available Green Open Access via the TU Delft Institutional Repository pursuant to Dutch Copyright Act (Article 25fa, the Taverne amendment). This provision does not affect copyright ownership.
Unless copyright is transferred by contract or statute, it remains with the copyright holder.

Sharing and reuse
Other than for strictly personal use, it is not permitted to download, forward or distribute the text or part of it, without the consent of the author(s) and/or copyright holder(s), unless the work is under an open content license such as Creative Commons.

Takedown policy
Please contact us and provide details if you believe this document breaches copyrights.
We will remove access to the work immediately and investigate your claim.

This work is downloaded from Delft University of Technology.

Green Open Access added to TU Delft Institutional Repository

'You share, we take care!' - Taverne project

https://www.openaccess.nl/en/you-share-we-take-care

Otherwise as indicated in the copyright section: the publisher is the copyright holder of this work and the author uses the Dutch legislation to make this work public.

24.2 A 1.66Gb/s and 5.8pJ/b Transcutaneous IR-UWB Telemetry System with Hybrid Impulse Modulation for Intracortical Brain-Computer Interfaces

Minyoung Song[1], Yu Huang[1,2], Yiyu Shen[1], Chengyao Shi[1,3], Arjan Breeschoten[1], Mario Konijnenburg[1], Huib Visser[1], Jac Romme[1], Barundeb Dutta[4], Morteza S. Alavi[2], Christian Bachmann[1], Yao-Hong Liu[1]

[1]imec-Netherlands, Eindhoven, The Netherlands
[2]Delft University of Technology, Delft, The Netherlands
[3]Eindhoven University of Technology, Eindhoven, The Netherlands
[4]imec, Leuven, Belgium

Intra-cortical extracellular neural sensing is being rapidly and widely applied in several clinical research and brain-computer interfaces (BCIs), as the number of sensing channels continues to double every 6 years. By distributing multiple high-density extracellular micro-electrode arrays (MEAs) *in vivo* across the brain, each with 1000's of sensing channels, neuroscientists have begun to map the correlation of neuronal activity across different brain regions, with single-neuron precision [1]. Since each neural sensing channel typically samples at 20 to 50kS/s with a >10b ADC, multiple MEAs demand a data transfer rate up to Gb/s [2]. However, these BCIs are severely hindered in many clinical uses due to the lack of a high-data-rate and miniature-wireless-telemetry solution that can be implanted below the scalp, i.e., transcutaneously (Fig. 24.2.1). The area of the wireless telemetry module should be miniaturized to ~3cm^2 due to neurosurgical implantation constraints. A transmission range up to 10cm is highly desirable, in order to improve the reliability of the wireless link against e.g., antenna misalignment, etc. Finally, the power consumption of the wireless telemetry should be limited to ~10mW to minimize thermal flux from the module's surface area, avoiding excessive tissue heating. Most of the conventional transcutaneous wireless telemetry systems adopt inductive coupling, but the data-rate is limited to a few Mb/s. A near-infrared (NIR) optical transcutaneous TX using a vertical-cavity-surface-emitting laser (VCSEL) [2] demonstrated a data-rate up to 300Mb/s but suffers from a limited transmission range (4mm) and requires a sub-mm precise alignment between the implant TX and a wearable RX. Impulse-radio UWB (IR-UWB) is promising for the targeted requirements [3-5].

This paper presents a transcutaneous IR-UWB TX with the highest data-rate, while achieving up to 10× longer transmission range compared to previously published works listed in Table 24.2.6, and with performance well within the volumetric and heat dissipation constraints. Three innovations are introduced: 1) a hybrid impulse modulation combining M-PPM, M-PSK and M-PAM for maximizing the link budget, 2) a power-efficient delay generator for a calibration-free M-PPM, 3) a low-noise 8-phase ring oscillator (RO) with duty-cycle correction for an accurate M-PSK. The state-of-the-art IR-UWB TX achieves 1.125Gb/s data-rate by adopting digitalized multi-pulse-position-modulation (D-MPPM) with a fine time step of ~50ps [3]. However, based on Euclidean distance, high Eb/N0 is required to discriminate between two adjacent pulse positions as the modulation order increases. This is not feasible in the targeted scenarios where the miniature antenna and tissue at UWB frequency can introduce up to 60dB of path loss. In this work, we propose a 3-D hybrid impulse modulation (4PAM-8PSK-4PPM) that employs an agile digital polar-based IR-UWB TX. This approach achieves high data-rate with a modulation order of 7, while significantly reducing the Eb/N0 requirement by ~20dB compared to M-PPM (Fig. 24.2.2). One key challenge of the proposed approach is to ensure a high level of independence among different modulations with low power overhead when performed simultaneously. Prior IR-UWB TXs perform impulse modulation with either carrier-less [3,4] or upconversion approaches [5]. The carrier-less TXs use edge-combining, which leverages the fast-switching digital logic in nanoscale CMOS, thus is power-efficient and requiring no dedicated LO. However, simultaneously performing M-PPM and M-PSK in carrier-less TXs is challenging, since both phase and time need to be modulated via delay edges. The classical IQ-based upconversion method can perform the high-order modulation, but is limited in achieving high energy efficiency. The polar-based upconversion TX [5] consumes low power, as the pulse shaping is performed asynchronously with delay cells and a digitally-controlled PA (DPA). However, it is limited to support only BPSK.

Figure 24.2.1 shows the proposed low-power polar-based IR-UWB TX capable of the hybrid impulse modulation. The impulse waveform is shaped by the DPA and a pulse shaper (PS) which uses delay cells to perform FIR filtering in the RF domain. An injection-locked RO (ILRO) is adopted to provide low jitter, 8 phases for 8PSK in a wide frequency range. A 7b 238MSym/s digital data is distributed to three different modulation paths, PAM, PSK, and PPM, after being synchronized with a 476MHz system clock (SYS_CLK). The switch-cap DPA with 32 unit cells supports up to 4PAM. The 8PSK is performed by selecting one of 8 phases from the ILRO using a phase selector (PHMUX). By accurately delaying the impulse with a PPM control (PPM_CTRL), precise 4PPM can be supported.

Figure 24.2.2 illustrates the timing diagram of the proposed 3-D hybrid impulse modulation. To avoid "inter-modulation" between PPM and PSK, the carrier phase is set at the beginning of each impulse symbol. To trigger an impulse, a 25% duty-cycled unit pulse (UNIT_PUL) at 238MHz is generated from the SYS_CLK. The PPM_CTRL shown in Fig. 24.2.2 modulates the delay of the UNIT_PUL according to the PPM data, and its output (PPM_OUT) is then fed to the PS to synthesize a triangular-shaped impulse. The pulse width of the impulse (T_{PULSE}) is set to ~2ns by the PS, and the symbol period (T_{SYMBOL}) is set by two cycles of the SYS_CLK to be 4.2ns. This ensures a sufficient time range (T_{PPM}) to perform 4PPM and avoids potential impact from inter-symbol interference or multi-path. The PPM time step (T_{PPM_STEP}) of 600ps is chosen according to the targeted Eb/N0 requirement (Fig. 24.2.2) and the PPM control complexity. The delay step is the quadruple of DCO_OUT (T_{DCO}). As long as the DCO is injection locked by the SYS_CLK, no extra delay calibration is required. The proposed PPM_CTRL only dissipates 115µW.

The proposed DCO is shown in Fig. 24.2.3. To reduce the antenna dimension and minimize harmonic pulling from the inductive powering [4], the DCO frequency is targeted to 6 to 9GHz, i.e., the high band of UWB. Generating 8 phases with an RO at up to 9GHz is challenging because it requires multiple delay stages for 8PSK. A negative skewing technique [6,7] is adopted for reducing the delay of each stage. In each delay cell, its PMOS (IPP/IPN) input is forwarded to the NMOS (INP/INN) one stage ahead, resulting in a faster transition and lower phase noise. However, this approach increases the duty-cycle error, which degrades the 8PSK accuracy. The proposed DCO buffer with a feedback duty-cycle correction is embedded in each delay cell with low capacitive loading and recovers the amplitude disturbance due to injection-locking, critical to ensure M-PAM accuracy. It can correct the duty-cycle error within 5ns, and each consumes only 120µW. The measured phase error of the proposed DCO is 2.6° at 6.7GHz, sufficient for low EVM (<-20dB) for 8PSK modulation.

The proposed UWB TX IC was fabricated in 28nm CMOS, occupying only 0.155mm^2, including an on-chip antenna matching network. The wireless module implemented on an FR4 PCB has a core electronic area of only 1.05cm^2, including a printed circular monopole antenna sized 9.4×7mm^2 and the TX IC (Fig. 24.2.7). The simulated antenna gain is -6 to -9dBi based on a human head model. An impulse modulation in the time domain, an "eye-diagram" of the impulse envelope and a constellation in the complex plane of the hybrid modulation are shown in Fig. 24.2.4, and demonstrate a high modulation quality. The DPA has a measured peak output power of 0dBm, and the measured DPA output spectrum complies to the FCC mask (Fig. 24.2.5), even without the attenuation of the tissue. To test the transmission range, the wireless module is inserted in a 15mm-thickness, multi-layer porcine tissue, placed at various distances away from a UWB RX composed of a 15cm^2 5dBi antenna, a 3dB-NF LNA and a high-speed oscilloscope as an ADC. The measured transmission ranges are 2 and 15cm at 1.66 and 1.43Gb/s data-rates, respectively, for bit-error-rate (BER) below 10^{-4}. Figure 24.2.6 summarizes the performance and benchmarks with state-ot-the-art transcutaneous and high-data-rate UWB TXs. The presented IR-UWB TX achieves the highest data-rate with longest range under the implant condition, leading to the best normalized energy-efficiency of 45pJ/bit/m among the other state-of-the-art entries in the table.

Acknowledgement:
This project has received funding from the European Research Council (ERC) under the European Union's Horizon 2020 research and innovation programme (grant agreement No. 101001448).

References:
[1] C. Stringer et al., "Spontaneous Behaviors Drive Multidimensional, Brain-Wide Activity," *Science*, vol. 36, no. 6437, April 2019.
[2] A. D. Marcellis et al., "A 300 Mbps 37 pJ/bit Pulsed Optical Biotelemetry," *IEEE TBioCAS*, vol.14, no.3, pp. 441-451, June 2020.
[3] G. Lee et al., "A 1.125Gb/s 28mW 2m-Radio-Range IR-UWB CMOS Transceiver," *ISSCC*, pp. 302-303, Feb. 2021.
[4] S. Mirbozorgi et al., " A Single-Chip Full-Duplex High Speed Transceiver for Multi-Site Stimulating and Recording Neural Implants," *IEEE TBioCAS*, vol.10, no.3, pp. 643-653, June 2016.
[5] E. Allebes et al., "A 3-to-10GHz 180pJ/b IEEE802.15.4z/4a IR-UWB Coherent Polar Transmitter in 28nm CMOS with Asynchronous Amplitude Pulse-Shaping and Injection-Locked Phase Modulation," *ISSCC*, pp. 304-305, Feb. 2021.
[6] S.-J. Lee et al., "A Novel High-Speed Ring Oscillator for Multiphase Clock Generation Using Negative Skewed Delay Scheme," *IEEE JSSC*, vol. 32, no. 2, pp. 289-291, Feb. 1997.
[7] M. Song, et al., "A 2.4 GHz 0.1-Fref-Bandwidth All-Digital Phase-Locked Loop With Delay-Cell-Less TDC," *IEEE TCAS-I*, vol.60, no.12, pp. 3145-3151, Dec. 2013.

2022 IEEE International Solid- State Circuits Conference (ISSCC) | 978-1-6654-2800-2/22/$31.00 ©2022 IEEE | DOI: 10.1109/ISSCC42614.2022.9731608

Authorized licensed use limited to: TU Delft Library. Downloaded on February 02,2023 at 10:05:26 UTC from IEEE Xplore. Restrictions apply.

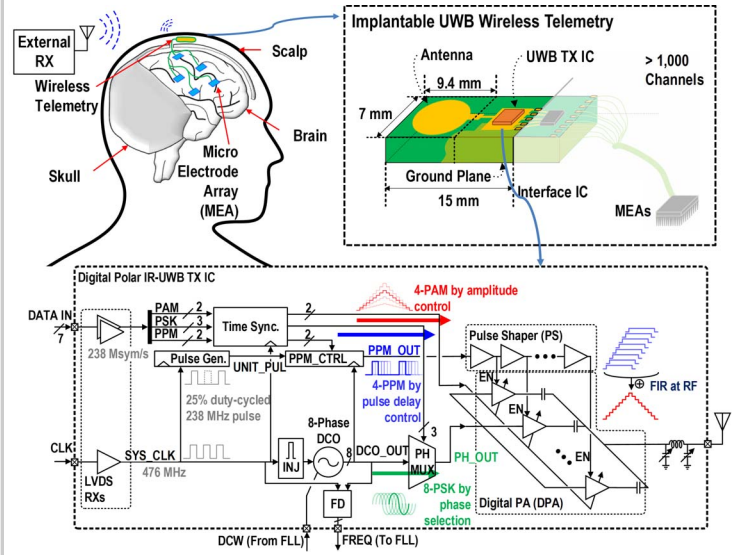


Figure 24.2.1: Conceptual diagram of intra-cortical neural sensing with 1.05cm² implantable UWB wireless telemetry (top) and block diagram of proposed UWB transmitter (TX).

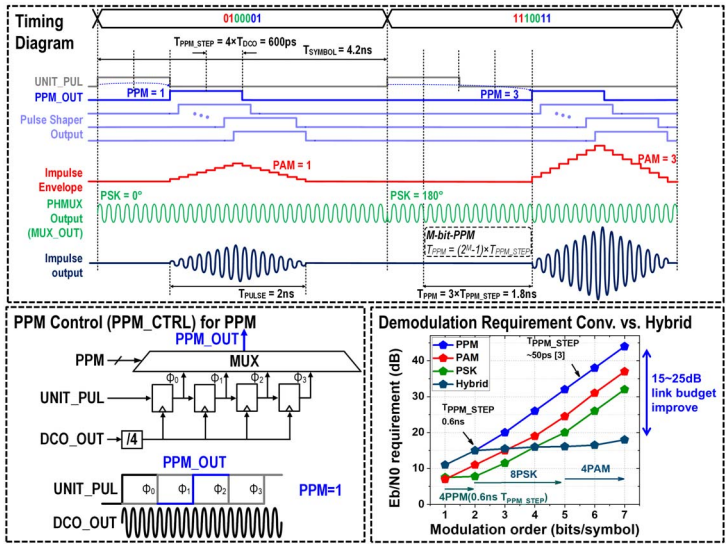


Figure 24.2.2: Timing diagram of the proposed 3-D hybrid modulation (top), proposed calibration-free PPM control circuit (bottom-left), and demodulation requirements for conventional modulations and proposed 3-D hybrid modulation (bottom-right).

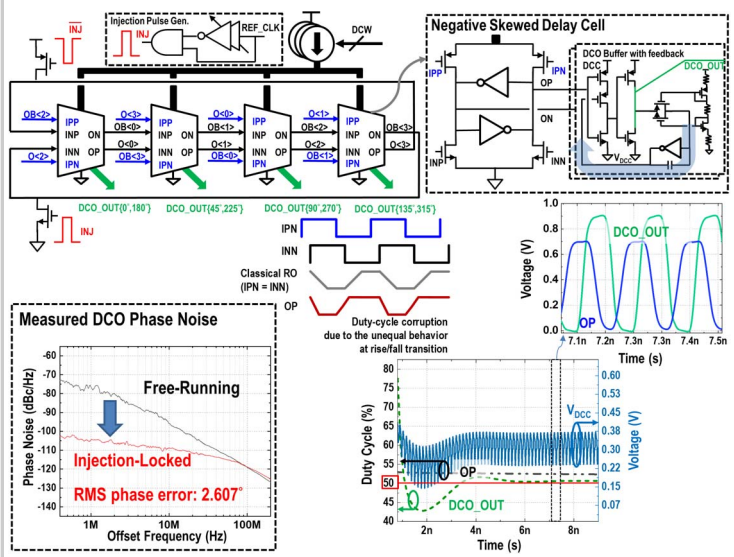


Figure 24.2.3: Proposed 8-phase DCO and its measured phase noise.

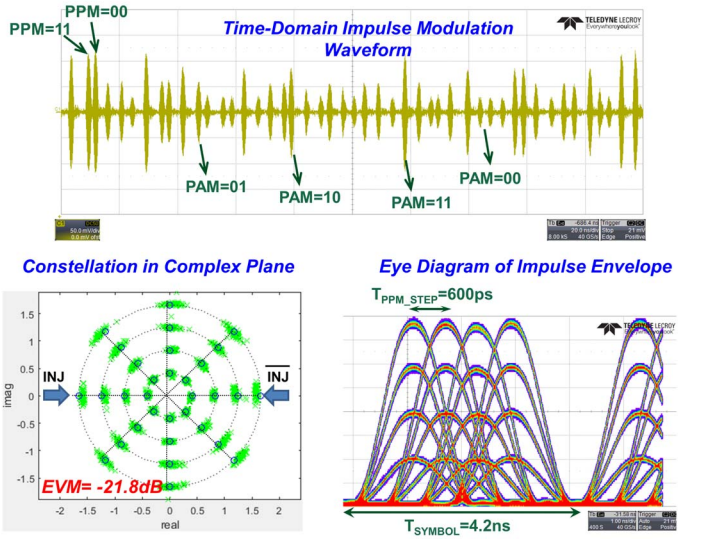


Figure 24.2.4: Measured time-domain impulse modulation waveform (top), constellation in complex plane (bottom-left), and envelope eye diagram of the proposed hybrid impulse modulation.

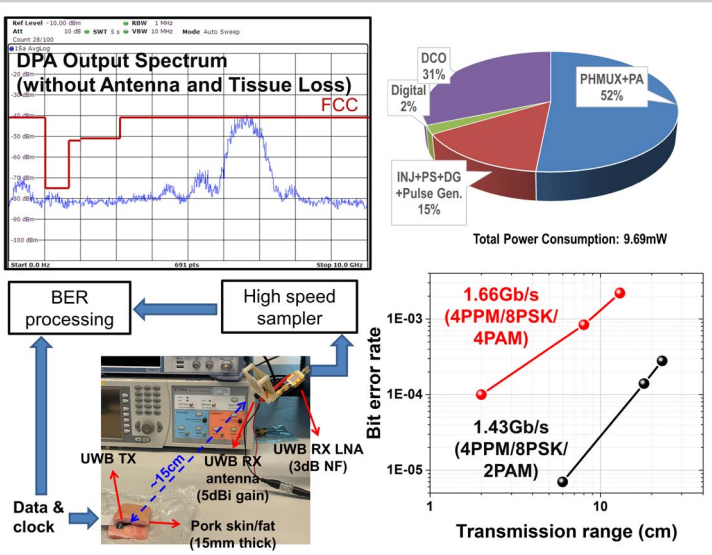


Figure 24.2.5: Measured spectrum at DPA out (top-left), power consumption (top-right), *in vitro* wireless measurement setup (bottom-left), and measured BER of 1.43Gb/s and 1.66Gb/s data-rates at various transmission ranges.

	This work	[4]	Ando, TBioCAS'16	[2]	[3]	[5]
Device technology	28nm CMOS	180nm CMOS	GaAs HBT	VCSEL	65nm CMOS	28nm CMOS
Wireless method	IR-UWB	IR-UWB	IR-UWB	Optical	IR-UWB	IR-UWB
Frequency	6-9GHz	3-7GHz	8GHz	NIR	4GHz	3-10GHz
Modulation	4PPM+8PSK+ 4PAM impulse	BPSK impulse	OOK impulse	OOK impulse	D-MPPM impulse	BPSK impulse
TX architecture	Digital polar (DPA+ PHMUX)	Edge combine	Edge combine	-	Edge combine	Digital polar (DPA+ ILRO)
Max. data rate	**1.66Gb/s**	500Mb/s	128Mb/s	300Mb/s	1.125Gb/s	27Mb/s
TX power cons.	9.69mW	5.4mW	561mW	11mW	28mW**	4.9mW
TX energy efficiency	**5.8pJ/b**	10.8pJ/b	438pJ/b	37pJ/b	25pJ/b**	180pJ/b
TX peak P_{OUT}	0dBm	N.A.	-12.3dBm	-	-10dBm	-0.7dBm
TX antenna area	66mm²	100mm²	N.A.	N.A.	N.A.	-
TX antenna gain	-8.5dBi	N.A.	N.A.	-	3dBi	-
Tissue thickness	15mm skin/fat	2mm skin/fat & 4mm bone	15-20mm phantom	3.5mm skin	No tissue	No tissue
Transmission range (in-vitro)	**2cm**@1.66Gb/s **15cm**@1.43Gb/s	1.5cm	1cm	0.4cm	N.A.***	-***
Normalized energy effi.*	**45pJ/b/m** (@1.43Gb/s)	720pJ/b/m	43.8nJ/b/m	9.25nJ/b/m	-	-

*TX energy efficiency normalized to 1m transmission range. **TX+RX
*** No transmission range reported with tissue or phantom.

Figure 24.2.6: Performance summary and comparison table with prior art.

Authorized licensed use limited to: TU Delft Library. Downloaded on February 02,2023 at 10:05:26 UTC from IEEE Xplore. Restrictions apply.

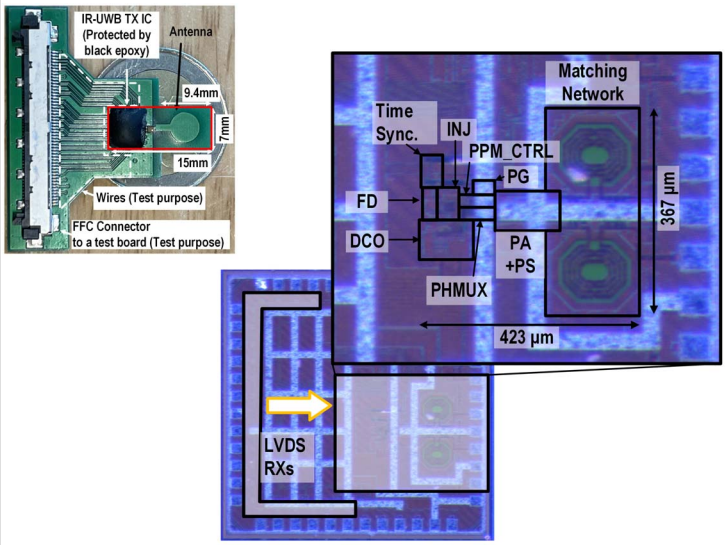


Figure 24.2.7: Die micrograph and prototype of the wireless module.

Authorized licensed use limited to: TU Delft Library. Downloaded on February 02,2023 at 10:05:26 UTC from IEEE Xplore. Restrictions apply.
978-1-6654-2800-2/22/$31.00 ©2022 IEEE